

Environmental engineering for quantum energy transport

Chikako Uchiyama^{1,2*} and William J. Munro^{3,4,2}, and Kae Nemoto²

¹*Graduate School of Interdisciplinary Research, University of Yamanashi,*

4-3-11, Takeda, Kofu, Yamanashi 400-8511, Japan

²*National Institute of Informatics, 2-1-2 Hitotsubashi, Chiyoda-ku, Tokyo 101-8430, Japan*

³*NTT Basic Research Laboratories, NTT Corporation,*

3-1 Morinosato-Wakamiya, Atsugi, Kanagawa 243-0198, Japan

⁴*Research Center for Theoretical Quantum Physics, NTT Corporation,*

3-1 Morinosato-Wakamiya, Atsugi, Kanagawa 243-0198, Japan

(Dated: May 19, 2022)

Transport phenomena are ubiquitous throughout the science, engineering and technology disciplines as it concerns energy, mass, charge and information exchange between systems. In particular, energy transport in the nanoscale regime has attracted significant attention within the physical science community due to its potential to explain complex phenomena like the electronic energy transfer in molecular crystals or the Fenna-Matthews-Olson / light harvesting complexes in photosynthetic bacteria with long time coherences. Energy transport in these systems is highly affected by environmental noise but surprisingly not always in a detrimental way. It was recently found that situations exist where noise actually enhances the transport phenomena. Such noise can take many forms, but can be characterised in three basic behaviours: quantum, coloured or nonlocal. All have been shown potential to offer an energy transport enhancement. The focus of this work is on quantum transport caused by stochastic environment with spatio-temporal correlation. We consider a multi-site nearest neighbour interaction model with pure dephasing environmental noise with coloured and nonlocal character and show how an accelerated rate for the energy transfer results especially under anti-correlation. Negative spatial correlations provide another control parameter to help one establish the most efficient transfer of energy and may provide new insights into the working of exciton transport in photosynthetic complexes. Further the usage of spatio-temporal correlated noise may be a beneficial resource for efficient transport in large scale quantum networks.

* hchikako@yamanashi.ac.jp

Introduction: Energy transport is a fundamental primitive in our world operating on length scales ranging from the nanometer scale to cosmological ones. It is at the core of natural life as well as our current technology. Any, even slight, improvements in transport efficiency can bring profound effects. In the natural world this can lead to a species dominating another, while in the technological world it can lead to lower energy consumption devices. Many of these improvements in the technological arena have been achieved by better device engineering reducing noise and imperfections. While this seems a perfectly logical approach, recently however it has been found, though nature already knew, that energy transport can be enhanced by adding environmental noise. This counter intuitive behaviour has shed new light on the conventional thinking that noises in transport phenomena should be removed, and it was indeed triggered by energy transport discussions of light harvesting complex of photosynthetic bacteria [1]. This leads to intensive investigations of four wave mixing in the Fenna-Matthews-Olson complex in green sulfur bacteria [2–4] or light harvesting complex in marine algae [5] or molecular crystals [6]. The striking long lived coherence in these experiments may only be explained by the positive effect of environmental noise. A simple theoretical model using pure dephasing as the environmental noise effect has shown that such noise can assist the excitation transport. This effect is termed environment-assisted quantum transport (ENAQT) [7] or dephasing-assisted transport [8]. The ENAQT model advanced the concept proposed by Haken and Strobl [9] who investigated the dynamics of exciton motion with delta-correlated stochastic noise (white noise). To describe the long-lived coherence observations, the model was extended to include finite noise correlation times and lengths. Several approaches were taken, including: (1) incorporating effects of coloured noise using dichotomic stochastic process [10] or a reservoir formed from an infinite number of quantum harmonic oscillators [11–15]; (2) incorporating finite correlation lengths [16–18]. Positive spacial correlations were shown to reduce the environmental effect, which can help the long-lived coherence. Both effects of temporal and spacial correlation together [19, 20] were shown to be beneficial, and recently an artificial realization of the ENAQT model has been proposed [21, 22]. The long-lived coherence means that the energy exchange between different sites remains for long time, however this may affect how fast we can transfer the energy. To tackle this issue of slow transfer, clues can be found in the spatial correlation of [17, 18]. Cao and Silbey [17] where the interaction between the sites is extended to include a phase relation and the dependence of transfer efficiency on the phase can be observed. In this case, the transfer efficiency is dependent on the period of the oscillation of the Bessel function defined spacial correlation [18]. These results imply that the phase relation between the dynamics of the sites can affect the transfer efficiency. This leads us to the natural question of what is the best spatio-temporal correlation function.

In this manuscript, we consider a simple multi-site model for the environment-assisted quantum transport using spatio-temporal correlated stochastic noise processes. The fundamental difference with the conventional treatment is to extend the spatial correlation into the negative region, i.e. anti-correlation, as well as including finite temporal correlations with exponential decay. For the two site model using the 2nd order of time-convolutionless (TCL) master equation, we analytically find that the time evolution of the population under negative spacial correlation is significantly faster than uncorrelated and positively correlated spacial noise. Extending the spacial correlations to include anti-correlations provides another control parameter to find efficient energy transfer regimes. Using two independent measures for transfer efficiency, we find a significant improvement in transported quantity and elapsed time for negative spacial correlation compared to noise with delta-correlation both in space and time as in the original ENAQT model. Extending to the three site model, we find that the negative spatial correlation between every other site shows the best transfer efficiency, while the negative correlation between the next nearest neighbors is worse.

Results

Model: Let us begin by considering a simple multi-site model for the environment-assisted quantum transport whose energy level diagram we schematically depict in Fig. (1). For N sites, the total Hamiltonian can be written as $\mathcal{H}(t) = \mathcal{H}_0 + g\mathcal{H}_1(t)$ with

$$\mathcal{H}_0 = \hbar \sum_{m=1}^N \omega_m |m\rangle\langle m| + \hbar \sum_{m < n} \Gamma_{nm} (|m\rangle\langle n| + |n\rangle\langle m|), \quad (1)$$

$$\mathcal{H}_1(t) = \hbar \sum_{m=1}^N f_m(t) |m\rangle\langle m|, \quad (2)$$

where g is an expansion parameter for the cumulant expansion of the time-convolutionless master equation with $|m\rangle$ the m -th excitation site, ω_m the m -th site Larmor frequency, Γ_{nm} the transition frequency between the m -th and n -th site, and $f_m(t)$ the fluctuating frequency on the m -th site which we consider here as stochastic process. We assume that the correlation function $\langle f_n(0)f_m(t) \rangle$ of this fluctuation can for convenience be described by a simple exponential

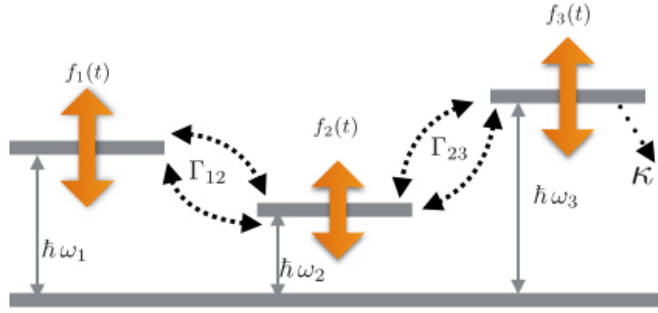


FIG. 1. Schematic energy level diagram of our multi-site system with the three site situation shown for illustrative purposes. Each site n has an associated excited state $|n\rangle$ with Larmor frequency ω_n and frequency fluctuation $f_n(t)$. Each site has a transition frequency Γ_{nm} between it and its adjacent site. The final site in the chain includes a probability κ to be trap the system in its ground state. This corresponds to the excitation leaving the chain.

decay as

$$\langle f_n(0)f_m(t) \rangle = c_{n,m} \Delta_{n,m}^2 \exp[-|t|/\tau_{c,\{n,m\}}], \quad (3)$$

where to allow for both positive and negative (anti) spatial correlations we introduce the quantity $c_{n,m}$ with $n, m = \{1, 2, \dots, N\}$. It is defined over the range by $-1 \leq c_{n,m} \leq 1$ with the extremal values -1 (+1) corresponding to perfectly anti-correlated (correlated) noise respectively. Next $\Delta_{n,m}$ and $\tau_{c,\{n,m\}}$ are the amplitude and correlation time of the fluctuation respectively. We also include damping with the rate κ at the end of the linear chain to trap the system in its ground state[17]. This corresponds to the excitation leaving the chain. Now averaging the density operator over the fluctuation using the time-convolutionless decomposition approach we obtain the master equation

$$\frac{d}{dt}\rho(t) = \langle \langle (-i\mathcal{L}_0) \rangle \rangle \rho(t) + \int_0^t (\langle \langle (-i\hat{\mathcal{L}}_1(0))(-i\hat{\mathcal{L}}_1(-\tau)) \rangle \rangle - \langle \langle (-i\hat{\mathcal{L}}_1(0)) \rangle \rangle \langle \langle (-i\hat{\mathcal{L}}_1(-\tau)) \rangle \rangle) d\tau \rho(t), \quad (4)$$

where $\mathcal{L}_0 X \equiv \frac{1}{\hbar}[\mathcal{H}_0, X]$ and $\mathcal{L}_1(t)X \equiv \frac{1}{\hbar}[\mathcal{H}_1(t), X]$ for an arbitrary operator X , and we define $\hat{\mathcal{L}}_1(t) = e^{i\mathcal{L}_0 t} \mathcal{L}_1(t) e^{-i\mathcal{L}_0 t}$. We have assumed that the average of the fluctuations is zero ($\langle f_\mu(t) \rangle = 0$ with $\mu = 0, 1$). The master equation given by (4) is inherently non-Markovian in nature and incorporates both spatial and temporal correlations. In the limit that such correlations vanish, a Markovian master equation is obtained (see Methods).

2 site model: As the description of our multi-site model has completed, let us now consider the simplest situation, $N = 2$. In the two-site model, the time evolution of the probability of finding the second site excited is shown in Fig. (2) when initially only the site 1 is fully excited. Fig. (2 a) represents the case where the fluctuation has no cross correlation between sites ($c_{n,m} = \delta_{n,m}$) with the inset which shows the short-time behavior. The uncorrelated situation (Fig. (2 a)) shows that there is an optimum time for the transported excitation to the second site depending on τ_c where we set the amplitude and correlation time of fluctuation at each site to be the same as $\Delta_{n,n} = \Delta$ and $\tau_{c,\{n,n\}} = \tau_c$ for $n = \{1, 2\}$. As the correlation time τ_c increases, the change of fluctuation carries a longer time memory effect and the optimum time decreases.

Next in Fig. (2 b) we consider the situation where the fluctuation is anti-correlated between the sites 1 and 2 by setting as $c_{1,2} = c_{2,1} = -1$. Assuming that the amplitude and correlation time of the fluctuation of each and between sites are the same, $\Delta_{n,m} = \Delta$ and $\tau_{c,\{n,m\}} = \tau_c$ for $n, m = \{1, 2\}$, we show in Fig. (2 b) that the transport finishes faster as the correlation time becomes longer. Comparing Fig. (2 a) with (2 b), we find that the anti-correlation between the sites makes transport to finish faster than the uncorrelated case. This is not unexpected when one examines the two time noise correlation function given by $\phi(t) = \langle (f_1(0) - f_2(0))(f_1(-\tau) - f_2(-\tau)) \rangle$. For uncorrelated noise this simplifies to $\langle f_1(0)f_1(-\tau) \rangle + \langle f_2(0)f_2(-\tau) \rangle = 2\langle f_1(0)f_1(-\tau) \rangle$, if the noise is the same for each site. For anti-correlated noise, the quantity becomes, $\phi(t) = 4\langle f_1(0)f_1(-\tau) \rangle$, to be twice the size of the uncorrelated case.

To quantify this improvement in more detail, let us examine two independent measures: (1) average trapping time and (2) ratio of transported quantity. The average trapping time [17] defined by $\langle t \rangle = \sum_n \tau_n$ with $\tau_n = \int_0^\infty dt \rho_{nn}(t)$ is plotted in Fig. (3 a) for varying degree of spatial correlation $c_{1,2} = c_{2,1} = c$. Since we are looking at a two-site situation, the trapping only at the second site with the rate κ leads to $\kappa \int_0^\infty dt \rho_{22}(t) = 1$ meaning the averaging time depends only on τ_c . This means that the transport feature depends on the correlation between sites. Especially, as c approaches to -1 , the average trapping time decreases, which shows that the transport finishes faster. Moreover, since the average trapping time is found to be inversely related to the quantum yield [17] given by $q \approx 1/(k_d \langle t \rangle + 1)$ where k_d is the decay constant (see Methods). The quantum yield becomes larger as c approaches to -1 .

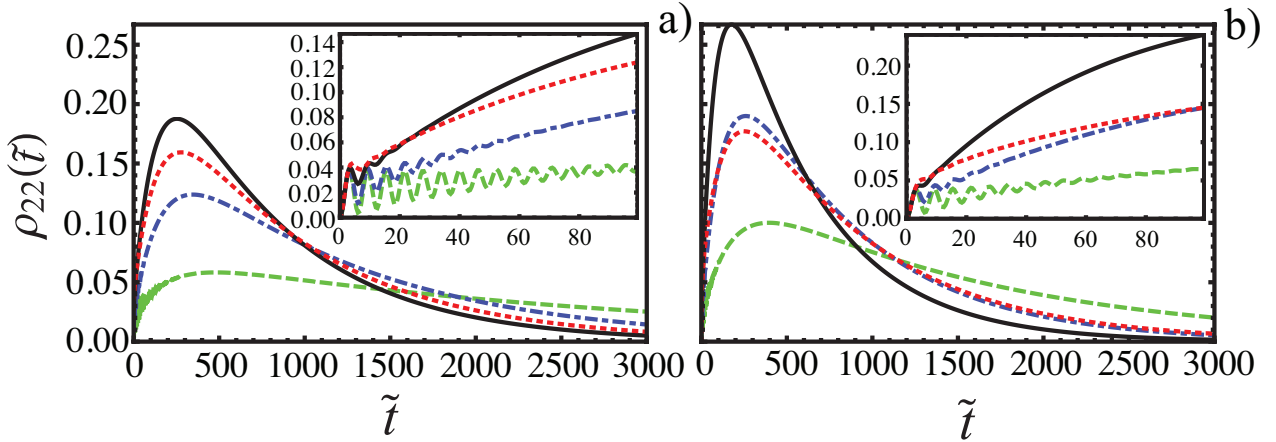


FIG. 2. Time evolution of $\rho_{22}(\tilde{t} = \Delta t)$ between energy fluctuation with spatially-uncorrelated noise, $c_{n,m} = \delta_{n,m}$, in a) and spatially-anti-correlated noise, $c_{n,m} = -1$, in b) for an initial condition $\rho_{11}(0) = 1$ with varying correlation time $\alpha = \Delta\tau_c$ as 0.1, 0.3, 1 and 10. The dashed lines corresponds to $\alpha = 0.1$, dotdashed lines to $\alpha = 0.3$, solid lines to $\alpha = 1$ and dotted lines to $\alpha = 10$. The system parameters are set as $g^2 = 0.1, \omega_1/\Delta = 1.5, \omega_2/\Delta = 0.5, \Gamma_{12}/\Delta = 0.1, \kappa/\Delta = 0.005$. The spatially-anti-correlated noise shows the acceleration of energy transport compared with the spatially-uncorrelated case.

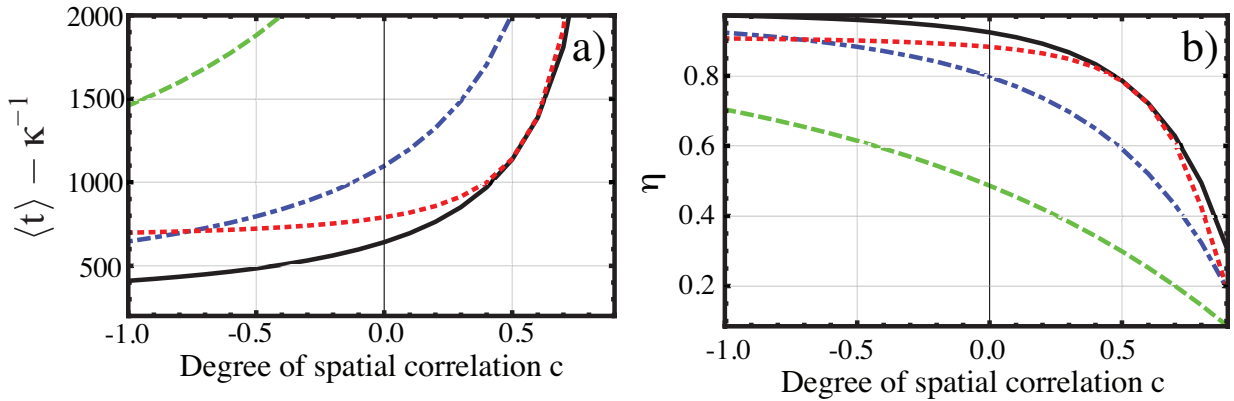


FIG. 3. Two-site transport properties and their dependence on the degree of spatial correlation. In a), we show the average trapping time and in b) the ratio of transported probability. In both situations, we find a monotonic dependence on degree of spatial correlation parameter c , which indicates that transport is mostly accelerated for the anti-correlated energy fluctuations. We show the dependence of both measures on the varying correlation time $\alpha = \Delta\tau_c$ as 0.1, 0.3, 1 and 10. The dashed lines corresponds to $\alpha = 0.1$, dotdashed lines to $\alpha = 0.3$, solid lines to $\alpha = 1$ and dotted lines to $\alpha = 10$. Focusing on the uncorrelated case, as α increases up to 1, the average trapping time (ratio of transported quantity) decreases (increases). But, for $\alpha = 10$, the former (the latter) increases (decreases), respectively, which shows that the suitable correlation time of fluctuation can accelerate the transport. While the average trapping time (ratio of transported quantity) increases (decreases), respectively, for the positive degree of correlation, we find the acceleration of transport as the degree becomes negative. Other parameters are the same as in Fig. (2).

Next, we introduce a quantity η to define an integrated probability that the excitation has been transported to the second site at a time t_u as

$$\eta = \kappa \int_0^{t_u} \rho_{22}(t') dt', \quad (5)$$

where the trapping rate κ is given by $\int_0^\infty \rho_{22}(t') dt' = \kappa^{-1}$. It is straightforward to observe from Figs. (2) and (3) the dependence of the energy transfer on both the degree of spatial correlation c and temporal correlation time $\alpha = \Delta\tau_c$. There is clearly a monotonic dependence on both our measures dependent on the degree of spatial correlation, with the best results occurring as we approach perfect anti-correlation ($\phi(t)$ is larger in this case). We also observe a non-monotonic dependence of the populations time evolution and the measures of transfer efficiency for temporal correlations. This means there will be a condition for optimal energy transfer on the correlation time. For small and

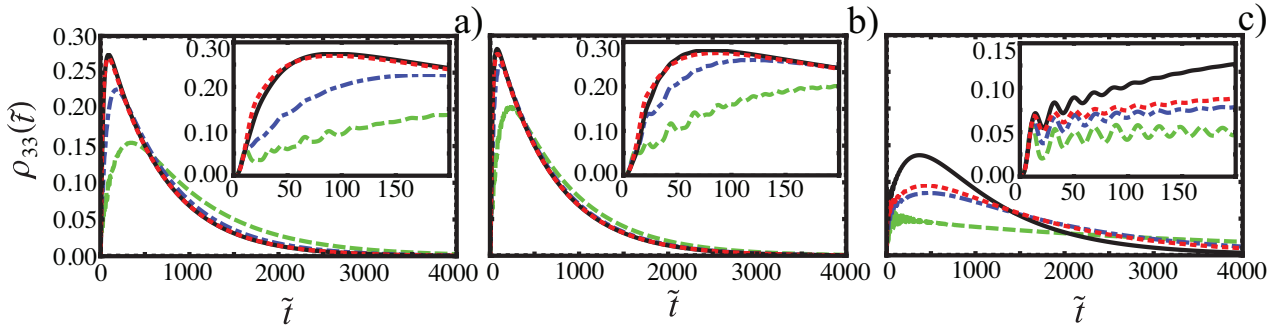


FIG. 4. Time evolution of $\rho_{33}(\tilde{t} = \Delta t)$ for the three site model under different degrees of spatial correlation: In a), we show the case for energy fluctuations with spatially-uncorrelated noise ($c_{n,m} = \delta_{n,m}$ for $n,m = \{1,2,3\}$) while b) shows the anti-correlated between nearest neighbor site case where $c_{1,2} = c_{2,1} = c_{2,3} = c_{3,2} = -1$ and positively correlated for site 1 and 3 $c_{1,3} = c_{3,1} = 1$. c) illustrates the case of anti-correlated between the site 1 and 3, and site 2 and 3, with $c_{1,3} = c_{3,1} = c_{2,3} = c_{3,2} = -1$ and correlated between the end $c_{1,2} = c_{2,1} = 1$. The dashed lines corresponds to $\alpha = 0.1$, dotdashed lines to $\alpha = 0.3$, solid lines to $\alpha = 1$ and dotted lines to $\alpha = 10$. The inset in each figure shows the short-time behavior. Comparing the behaviour between the different case, we find that the "anti-ferromagnetic" correlation (case b) accelerates the transport most. We have set the parameters as, we set $\omega_1/\Delta = 1.5, \omega_2/\Delta = 1.2, \omega_3/\Delta = 1.0, V/\Delta = 0.1$ and $\kappa/\Delta = 0.005$ while other parameters are the same as in Fig. (2).

decreasing α , the energy transfer takes longer time due to the fact that fluctuation becomes too fast making it difficult for the energy gaps to be close and the transition probability between sites becomes smaller (this moves us towards the Markovian limit). However for α larger than the optimal value, the correlation time becomes larger making the transition probability smaller again. Thus for the best performance one should operate near this optimal value.

3-site model. The two-site model has shown how spatial correlations are potentially an important resource for efficient energy transfer. The natural question which follows to this would be whether this is true for when the system has more than two sites. We extend the model to three-site linear chain under the nearest neighbor interaction with the interaction strengths given by $\Gamma_{12} = \Gamma_{21} = \Gamma_{23} = \Gamma_{32} = V$ and $\Gamma_{13} = \Gamma_{31} = 0$. In Fig. (4) we plot the time evolution of the population of the third (final) site $\rho_{33}(\tilde{t})$ for spatially-uncorrelated noise and two spatially-anti correlated noise cases. Fig.(4 a) corresponds to the uncorrelated case with $c_{n,m} = \delta_{n,m}$ for $n, m = \{1, 2, 3\}$, while Fig. (4 b) represents the case for the anti-correlated noise between the nearest neighbor sites with $c_{1,2} = c_{2,1} = c_{2,3} = c_{3,2} = -1$ and correlated between the end sites $c_{1,3} = c_{3,1} = 1$. Finally, Fig. (4 c) represents the case for the anti-correlated noise between the sites 1 and 3, and the sites 2 and 3, with $c_{1,3} = c_{3,1} = c_{2,3} = c_{3,2} = -1$ and correlated between the sites 1 and 2, $c_{1,2} = c_{2,1} = 1$. In each sub-figure, we find that the dependence of the dynamics on the correlation time for the two-site model remains for the three-site case: transport finishes faster as the correlation time becomes longer. Comparing Fig.(4 a, b, c), we find that the anti-correlated between the nearest neighbor sites shows the most effective transport.

To explore these features systematically, we evaluate the average trapping time $\langle t \rangle$. In Fig.(5), we show the contour plot of dependence of $\langle t \rangle - \kappa^{-1}$ on changing the degree of correlation $c_{n,m}$. Comparing Fig.(5 a,b), we find that "anti-ferromagnetic" correlation where the fluctuation is anti-correlated between the nearest neighbor site shows the most effective transport. The physical origin of such a feature arises from the fact that the transition probability between the nearest neighbor is largest with anti-correlation (as illustrated in the two site case). This corresponds to the "anti-ferromagnetic" correlation in the three site model. Here the average trapping time $\langle t \rangle$ for the uncorrelated case is $\sim 12\%$ larger than the "anti-ferromagnetic" case. This clearly shows the acceleration in the energy transport occurs with "anti-ferromagnetic" correlations. However, the difference is smaller as α increases (5 % for $\alpha = 0.5$).

Discussion and Conclusion

Energy transport in molecular complexes / light harvesting complexes in photosynthetic bacteria has raised many fundamental questions about how our nature operates and challenged our intuition about the fundamental role of noise in such processes. It was recently found that noise can actually enhance such transport phenomena through temporally correlated [11–15] or spatially correlated fluctuations [18]. In this work we have considered the transport of quantum energy for a multi-site linear chain model whose energy levels are affected by spatio-temporal correlated stochastic noise processes [16, 17]. We find that the energy transport can be accelerated by extending the spatial correlation into the negative region (anti-correlation). In the two-site model, our numerical analysis showed the

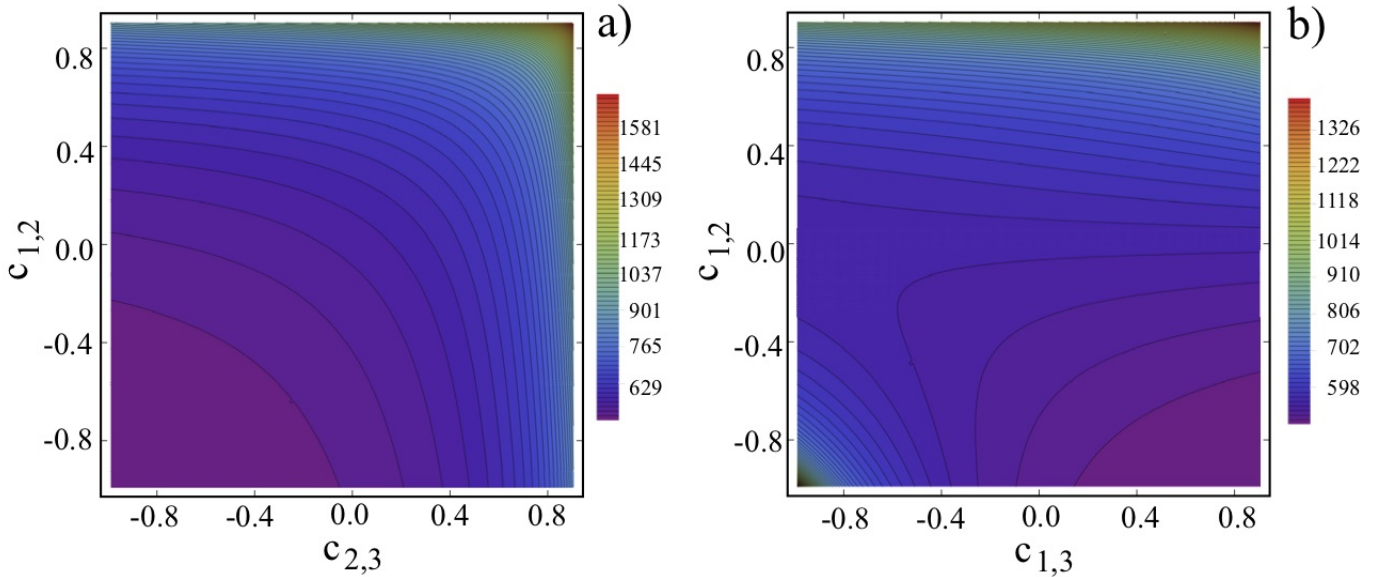


FIG. 5. Average trapping time $\langle t \rangle - \kappa^{-1}$ for three-site transport depending on the degree of spatial correlation for $\alpha = 0.3$. a) shows this quantities dependency on $c_{2,3} (= c_{3,2})$ and $c_{1,2} (= c_{2,1})$ while setting $c_{1,3} = c_{3,1} = c_{2,3}c_{1,2}$. Similarly b) shows our quantities dependency on $c_{1,3} (= c_{3,1})$ and $c_{1,2} (= c_{2,1})$ while setting $c_{2,3} = c_{3,2} = c_{1,3}c_{1,2}$. Other parameters are the same as in Fig. (4). The shorter values of average trapping time occurs at the left hand bottom side corner in a) and right hand bottom side corner in b). This means the “anti-ferromagnetic” correlation case is the best choice for acceleration of transport in this case.

significant acceleration in the energy transfer with the negative spacial correlation. By extending the model to three sites, we generalized this tendency of the efficient energy transfer by showing optimal efficiencies for the “anti-ferromagnetic” correlation. For the temporal correlation dependencies, we explored the energy transfer dependence by changing the parameter $\alpha = \Delta\tau_c$. We found a non-monotonic dependence on the population time evolution and our transfer efficiency measures, and hence an optimum condition for energy transfer dependent on the correlation time exists. These results show new possibilities to understand efficient energy transport in nature and implement it in technologies by engineering of the environment spacial and temporal characteristics.

Acknowledgements We would like to thank Ryuta Tezuka, Ryuji Nakamura, Shun Imazawa, and Dr. Kazunari Hashimoto for valuable discussions. This work was supported in part from the MEXT KAKENHI Grant-in-Aid for Scientific Research on Innovative Areas Science of hybrid quantum systems Grant No.15H05870, JSPS KAKENHI Grant Numbers 15K05200, and the researcher exchange promotion program of the Research Organization of Information and Systems.

Author Contributions

All authors researched, collated, and wrote this paper.

Competing Interests

The authors declare no conflict of interest.

[1] Blankenship, R. E. *Molecular Mechanisms of Photosynthesis* (Blackwell Science: Oxford/Malden, 2002).
[2] Brixner, T. et. al. Two-dimensional spectroscopy of electronic couplings in photosynthesis. *Nature* **434**, 625 (2005).
[3] Lee, H. Cheng, Y.-C. Fleming, G. R. Coherence dynamics in photosynthesis: protein protection of excitonic coherence. *Science* **316**, 1462 (2007).
[4] Panitchayangkoon, G. et. al. Long-lived quantum coherence in photosynthetic complexes at physiological temperature. *Proc. Nat. Sci.* **107**, 12766 (2010).
[5] Collini, E. et. al. Coherently wired light-harvesting in photosynthetic marine algae at ambient temperature. *Nature* **463**, 644 (2010).

- [6] Collini, E. and Scholes, G. D. Coherent intrachain energy migration in a conjugated polymer at room temperature. *Science* **323**, 369 (2009).
- [7] Rebentrost, P. Mohseni, M. Kassal, I. Lloyd, S. and Aspuru-Guzik, A. Environment-assisted quantum transport. *tNew J. Phys.* **11**, 033003 (2009).
- [8] Plenio, M. B. and Huelga, S. F. Dephasing-assisted transport: quantum networks and biomolecules. *New J. Phys.* **10**, 113019 (2008).
- [9] Haken, H. and Strobl, G. An exactly solvable model for coherent and incoherent exciton motion. *Z. Phys.* **262**, 135 (1973).
- [10] Chen, X. and Silbey, R. J. Excitation energy transfer in a non-Markovian dynamical disordered environment: Localization, narrowing, and transfer efficiency. *J. Phys. Chem. B* **115**, 5499 (2011).
- [11] Ishizaki, A. and Fleming, G. R. On the adequacy of the Redfield equation and related approaches to the study of quantum dynamics in electronic energy transfer. *J. Chem. Phys.* **130**, 234110 (2009).
- [12] Ishizaki, A. and Fleming, G. R. Unified treatment of quantum coherent and incoherent hopping dynamics in electronic energy transfer: Reduced hierarchy equation approach. *J. Chem. Phys.* **130**, 234111 (2009).
- [13] Rebentrost, P. Chakraborty, R. and Aspuru-Guzik, A. Non-Markovian quantum jumps in excitonic energy transfer. *J. Chem. Phys.* **131**, 184102 (2009).
- [14] Mohseni, M. Shabani, A. Lloyd, S. Omar, Y. and Rabitz, H. Geometrical effects on energy transfer in disordered open quantum systems. *J. Chem. Phys.* **138**, 204309 (2013).
- [15] Jeske, J. Ing, D. J. Plenio, M. B. Huelga, S. F. and Cole, J. H. Bloch-Redfield equations for modeling light-harvesting complexes. *J. Chem. Phys.* **142**, 064104 (2015).
- [16] Yu, Z. G. Berding, M. A. and Wang, H. Spatially correlated fluctuations and coherence dynamics in photosynthesis. *Phys. Rev. E* **78**, 050902(R) (2009).
- [17] Cao, J. and Silbey, R. J. Optimization of exciton trapping in energy transfer processes. *J. Phys. Chem. A* **113**, 13825 (2009).
- [18] Fassioli, F. Nazir, A. and Olaya-Castro, A. Quantum state tuning of energy transfer in a correlated environment. *J. Phys. Chem. Lett.* **1**, 2139 (2010).
- [19] Wu, J. Liu, F. Shen, Y. Cao, J. and Silbey, R. J. Efficient energy transfer in light-harvesting systems, I: Optimal temperature, reorganization energy and spatial-temporal correlations. *New J. Phys.* **12**, 105012 (2010).
- [20] Sarovar, M. Cheng, Y.-C. and Whaley, K. B. Environmental correlation effects on excitation energy transfer in photosynthetic light harvesting. *Phys. Rev. E* **83**, 011906 (2011).
- [21] Levi, L. Krivolapov, Y. Fishman, S. and Segev, M. Hyper-transport of light and stochastic acceleration by evolving disorder. *Nat. Phys.* **8**, 912 (2012).
- [22] Biggerstaff, D. N. et. al. Enhancing quantum transport in a photonic network using controllable decoherence. *Nat. Comm.* **7**, 11282 (2016).
- [23] Gorini, V. Kossakowski, A. and Sudarshan, E. C. G. Completely positive dynamical semigroups of N-level systems. *J. Math. Phys.* **17**, 821 (1976).
- [24] Lindblad, G. On the generators of quantum dynamical semigroups. *Commun. Math. Phys.* **48**, 119 (1976).
- [25] Kubo, R. Stochastic Liouville equations. *J. Math. Phys.* **4**, 174 (1963).
- [26] Hänggi, P. and Thomas, H. Time evolution, correlations and linear response of non-Markov processes, *Z. Phys. B: Condens. Matter* **26**, 85 (1977).
- [27] Hashitsume, N. Shibata, F. and Shingu, F. Quantal master equation valid for any time scale. *J. Stat. Phys.* **17**, 155 (1977).
- [28] Kubo, R. Toda, M. and Hashitsume, N. *Statistical Physics II*, (Springer-Verlag, New York, 1985).
- [29] Shibata, F. Takahashi, F. and Hashitsume, N. A generalized stochastic liouville equation. Non-Markovian versus memoryless master equations. *J. Stat. Phys.* **17**, 171 (1977).
- [30] Chaturvedi, S. and Shibata, F. Time-convolutionless projection operator formalism for elimination of fast variables. Applications to Brownian motion. *Z. Phys. B: Condens. Matter* **35**, 297 (1979).
- [31] Shibata, F. and Arimitsu, T. Expansion formulas in nonequilibrium statistical mechanics. *J. Phys. Soc. Jpn.* **49**, 891 (1980).
- [32] Uchiyama, C. and Shibata, F. Unified projection operator formalism in nonequilibrium statistical mechanics. *Phys. Rev. E* **60**, 2636 (1999).
- [33] Breuer, H. -P. and Petruccione, F. *The Theory of Open Quantum Systems* (Oxford University Press, New York, 2002).
- [34] Fruchtman, A. Lambert, N. and Gauger, E. M. When do perturbative approaches accurately capture the dynamics of complex quantum systems. *Sci. Rep.* **6**, 28204 (2016).

Methods

An open systems approach: As shown in Fig (1) our multi-site model contains fluctuating excited state energy levels as well as an energy trap on the last site (energy decay). In principle this means an open systems approach must be used - especially as our energy level fluctuations are stochastic in nature. It would thus be natural to write down a master equation in Lindblad form[23, 24] (which can easily handle the last site energy decay), which would force us to use a white noise model where the fluctuations are not correlated in time. However in this case we want to examine temporal and spacial correlation effects. This means the typical master equation is not appropriate, however a master equation can be derived using time-convolutionless decomposition techniques [25–33].

Derivation of the time convolution type of master equation:

The master equation given by Eq.(4) is obtained by extracting the time evolution of the excitations in each site from the one of the total system which is written by the Liouville-von Neuman equation as

$$\frac{d}{dt}W(t) = -i\mathcal{L}(t)W(t), \quad (6)$$

where $W(t)$ is the density operator for the total system and $\mathcal{L}(t)$ is the Liouville operator defined as $\mathcal{L}(t)X = \frac{1}{\hbar}[\mathcal{H}(t), X]$ for an arbitrary operator X . In such a case, the extraction averages $W(t)$ over the stochastic process of the fluctuation. Our purpose is to obtain the time evolution of the reduced density operator $\langle W(t) \rangle (\equiv \rho(t))$ where we denote the average operation as $\langle \dots \rangle$. For this purpose, it is convenient to use the projection operator method[25–33]. Introducing a projection operator, \mathcal{P} , which is an idempotent operator with a property as $\mathcal{P}^2 = \mathcal{P}$, we describe the reduced density operator as $\mathcal{P}W(t) \equiv \langle W(t) \rangle (\equiv \rho(t))$. To obtain the time evolution of $\mathcal{P}W(t)$, we use the formal solution of Eq. (6) as $W(t) = U_+(t, t_0)W(t_0)$ with $U_+(t, t_0) = T_+ \exp[-i \int_{t_0}^t \mathcal{L}(\tau) d\tau]$ where T_+ is an increasing time ordering operator from the right to the left. The procedure to obtain the master equation, Eq.(4), is roughly divided into the following six steps:

1. First we define the relevant \mathcal{P} part and the irrelevant $\mathcal{Q} (\equiv 1 - \mathcal{P})$ part of the time evolution operator $\hat{U}_+(t, t_0)$ as

$$x(t) \equiv \mathcal{P}\hat{U}_+(t, t_0), \quad y(t) \equiv \mathcal{Q}\hat{U}_+(t, t_0), \quad (7)$$

where we use interaction picture with the definition as $\hat{U}_+(t, t_0) = e^{-i\mathcal{L}_0(t-t_0)}U_+(t, t_0) = T_+ \exp[-\int_{t_0}^t dt' i\hat{\mathcal{L}}_1(t') dt']$ and $\hat{\mathcal{L}}_1(t) = e^{i\mathcal{L}_0(t-t_0)}\mathcal{L}_1(t)e^{-i\mathcal{L}_0(t-t_0)}$.

2. Then we derive simultaneous differential equations for $x(t)$ and $y(t)$ as

$$\frac{d}{dt}x(t) = \mathcal{P}(-i\hat{\mathcal{L}}_1(t))x(t) + \mathcal{P}(-i\hat{\mathcal{L}}_1(t))y(t), \quad (8)$$

$$\frac{d}{dt}y(t) = \mathcal{Q}(-i\hat{\mathcal{L}}_1(t))x(t) + \mathcal{Q}(-i\hat{\mathcal{L}}_1(t))y(t). \quad (9)$$

3. Next the formal solution of the irrelevant \mathcal{Q} part can be written as,

$$y(t) = \int_{t_0}^t V_+(\tau) \mathcal{Q}(-i\hat{\mathcal{L}}_1(\tau))x(\tau) d\tau + V_+(t, t_0)\mathcal{Q}. \quad (10)$$

with $\hat{V}_+(t, \tau) = T_+ \exp[-i \int_{\tau}^t \mathcal{Q}\hat{\mathcal{L}}_1(\tau') d\tau']$.

4. We then rewrite $x(\tau)$ in Eq. (10) with $x(t)$ and $y(t)$ using the relation

$$x(\tau) = \mathcal{P}\hat{U}_+(\tau, t_0) = \mathcal{P}\hat{U}_-(t, \tau)(x(t) + y(t)), \quad (11)$$

where $\hat{U}_-(t, t_0) = T_- \exp[i \int_{t_0}^t \hat{\mathcal{L}}_1(\tau') d\tau']$ with T_- an increasing time ordering operator from the left to the right. The formal solution of $y(t)$ has the form

$$y(t) = \theta(t)^{-1}((1 - \theta(t))x(t) + \hat{V}_+(t, t_0)\mathcal{Q}), \quad (12)$$

where we define

$$\theta(t) = 1 - \int_{t_0}^t \hat{V}_+(\tau) \mathcal{Q}(-i\hat{\mathcal{L}}_1(\tau))\mathcal{P}\hat{U}_-(t, \tau) d\tau \equiv 1 - \sigma(t). \quad (13)$$

5. Next we substitute the formal solution of $y(t)$ into Eq. (8) and multiply $W(t_0)$ from the right on the both hand sides of Eq. (8),

$$\frac{d}{dt}\hat{\rho}(t) = \mathcal{P}(-i\hat{\mathcal{L}}_1(t))\hat{\rho}(t) + \Xi(t, t_0)\hat{\rho}(t) + I(t, t_0)W(t_0), \quad (14)$$

with $\hat{\rho}(t) = e^{-i\mathcal{L}_0(t-t_0)}\rho(t)$, $\Xi(t, t_0) = \mathcal{P}(-i\hat{\mathcal{L}}_1(t))(1 - \theta(t)^{-1})$ and $I(t, t_0) = \mathcal{P}(-i\hat{\mathcal{L}}_1(t))\theta(t)^{-1}\hat{V}(t, t_0)\mathcal{Q}$.

6. Eq. (14) is then expanded with using the relation as $\theta(t)^{-1} = \sum_{n=0}^{\infty} \sigma(t)^n$. This gives

$$\frac{d}{dt} \hat{\rho}(t) = \mathcal{P}(-i\hat{\mathcal{L}}_1(t))\hat{\rho}(t) + \mathcal{P}(-i\hat{\mathcal{L}}_1(t)) \sum_{n=1}^{\infty} \sigma(t)^n \hat{\rho}(t) + I(t, t_0)W(t_0), \quad (15)$$

7. Expansion of Eq. (15) up to the second order of cumulant for $\mathcal{L}_1(t)$ with using an assumption as $\langle f_m(t) \rangle = 0$ and $\mathcal{Q}W(t_0) = 0$ and transformation into the original picture from the interaction picture gives Eq.(4).

Now let us consider the specific example, two site model.

TCL type master equation for the 2-site model:

The concrete form of the master equation for the two-site model is written as

$$\begin{aligned} \frac{d}{dt} \rho_{11}(t) &= -i\Gamma_{12}(-\rho_{12}(t) + \rho_{21}(t)), \\ \frac{d}{dt} \rho_{12}(t) &= -i\{\Gamma_{12}(-\rho_{11}(t) + \rho_{22}(t)) + (\omega_1 - \omega_2)\rho_{12}(t)\} - g^2\{F_1(\omega_1, \omega_2, \Gamma_{12}, t)(\rho_{11}(t) - \rho_{22}(t)) + F_2(\omega_1, \omega_2, \Gamma_{12}, t)\rho_{12}(t)\}, \\ \frac{d}{dt} \rho_{21}(t) &= -i\{\Gamma_{12}(\rho_{11}(t) - \rho_{22}(t)) - (\omega_1 - \omega_2)\rho_{21}(t)\} - g^2\{F_1^*(\omega_1, \omega_2, \Gamma_{12}, t)(\rho_{11}(t) - \rho_{22}(t)) + F_2(\omega_1, \omega_2, \Gamma_{12}, t)\rho_{21}(t)\}, \\ \frac{d}{dt} \rho_{22}(t) &= -i\Gamma_{12}(\rho_{12}(t) - \rho_{21}(t)) - \kappa\rho_{22}(t), \end{aligned}$$

where $\rho_{nm}(t)$ is the (n, m) element of the reduced density operator $\rho(t)$, κ is the trap frequency at the 2nd site and we $F_n(\omega_1, \omega_2, \Gamma_{12}, t)$ for $n = 1, 2$ are defined as

$$F_1(\omega_1, \omega_2, \Gamma_{12}, t) = - \int_0^t d\tau \left(\frac{\Gamma_{12}(\omega_1 - \omega_2)}{\mu^2} (1 - \cos(\mu\tau)) - i \frac{\Gamma_{12}}{\mu} \sin(\mu\tau) \right) \phi(\tau), \quad (16)$$

$$F_2(\omega_1, \omega_2, \Gamma_{12}, t) = \int_0^t d\tau \left(\left(\frac{(\omega_1 - \omega_2)}{\mu} \right)^2 + (1 - \left(\frac{(\omega_1 - \omega_2)}{\mu} \right)^2) \cos(\mu\tau) \right) \phi(\tau), \quad (17)$$

with

$$\mu = \sqrt{(\omega_1 - \omega_2)^2 + 4\Gamma_{12}^2}, \quad (18)$$

$$\phi(t) = \langle (f_1(0) - f_2(0))(f_1(-t) - f_2(-t)) \rangle. \quad (19)$$

In Eq. (19), $\langle f_n(0)f_m(-\tau) \rangle$ with $n, m = \{1, 2\}$ is the correlation function of the fluctuation of the frequency. The obtained master equation shows that the transport is controlled by adjusting correlation function of the fluctuation on each site as well as the one between the fluctuation on the different site such as $\langle f_1(0)f_2(-\tau) \rangle$. Assuming that the amplitude and correlation time of the fluctuation of each and between site are the same, $\Delta_{n,m} = \Delta$ and $\tau_{c,\{n,m\}} = \tau_c$ for $n, m = \{1, 2\}$, $\phi(t)$ in Eq. (19) is given by $\phi(t) = 4\langle f_1(0)f_1(-t) \rangle$ for anti-correlated case ($c = -1$) and $\phi(t) = 2\langle f_1(0)f_1(-t) \rangle$ for the uncorrelated case ($c = 0$).

The dynamics described by time convolutionless(TCL) type of master equation is compared to the one by hierarchical equations of motion (HEOM) for the spin-boson system in [34] where they find that the second order and fourth order of TCL equation and HEOM shows almost the same dynamics for weak coupling case.

Relation with the traditional Lindblad master equation:

The TCL master equation given by Eq.(4) in a specific limit reduces to the typical Lindblad master equation. In such a case we set the upper integral limit $t \rightarrow \infty$ giving

$$\frac{d}{dt} \rho(t) = \langle \langle (-i\mathcal{L}_0) \rangle \rangle \rho(t) + \int_0^{\infty} (\langle \langle (-i\hat{\mathcal{L}}_1(0))(-i\hat{\mathcal{L}}_1(-\tau)) \rangle \rangle - \langle \langle (-i\hat{\mathcal{L}}_1(0)) \rangle \rangle \langle \langle (-i\hat{\mathcal{L}}_1(-\tau)) \rangle \rangle) d\tau \rho(t), \quad (20)$$

where all of the coefficients are time-independent. This is the Born-Markov approximation[27, 28, 33]. For example, the time-dependent coefficients of the two site model ignoring spacial correlation ($c = 0$) can be approximated as

$$\begin{aligned} F_1(\omega_1, \omega_2, \Gamma_{12}, \infty) &= -2\Delta^2 \left(\frac{\Gamma_{12}(\omega_1 - \omega_2)\tau_c^3}{1 + \mu^2\tau_c^2} - i \frac{\Gamma_{12}\tau_c^2}{\mu^2\tau_c^2 + 1} \right) \\ F_2(\omega_1, \omega_2, \Gamma_{12}, \infty) &= 2\Delta^2 \left(\frac{\tau_c}{1 + \mu^2\tau_c^2} + \left(\frac{(\omega_1 - \omega_2)}{\mu} \right)^2 \frac{\mu^2\tau_c^3}{1 + \mu^2\tau_c^2} \right), \end{aligned} \quad (21)$$

Taking the limit of the correlation time τ_c to approach zero with maintaining $\Delta^2\tau_c$ finite [28], we obtain

$$\lim_{\tau_c \rightarrow 0} F_1(\omega_1, \omega_2, \Gamma_{12}, \infty) = 0, \quad \lim_{\tau_c \rightarrow 0} F_2(\omega_1, \omega_2, \Gamma_{12}, \infty) = 2 \frac{\Delta^2 \tau_c}{1 + \mu^2 \tau_c^2}, \quad (22)$$

Defining $\lim_{\tau_c \rightarrow 0} F_2(\omega_1, \omega_2, \Gamma_{12}, \infty) \equiv \gamma$, our master equation given by Eq.(4) reduces to the Lindblad form[23, 24] :

$$\frac{d}{dt} \rho(t) = -\frac{i}{\hbar} [\mathcal{H}_0, \rho(t)] + \frac{\gamma}{2} \sum_m [2A_m \rho(t) A_m^\dagger - A_m A_m^\dagger \rho(t) - \rho(t) A_m A_m^\dagger], \quad (23)$$

where $A_m = |m\rangle\langle m|$. We find that Eq. (23) is the same as the master equation obtained in [7] for the Haken-Strobl model. Moreover, when we substitute the stationary value of $\rho_{12}(t)$ into the differential equation, we obtain the same differential equation as in [17]. Besides the above, let us note that, by using the time convolutionless type of master equation, we need only to take long-time limit as the approximation procedure, which is much simpler than using the time-nonlocal (time-convolution) type of master equation[27].

Numerical methods:

The effect of the fluctuation on the time evolution of the density operator is described with the time dependent coefficient of the second term in the right hand side of the time-convolutionless type of master equation given by Eq. (4). To obtain the time evolution of the density operator, we numerically solved the master equation by evaluating the time dependent coefficient and iterating the equation step by step with the coefficient. In the evaluation, we scaled the time variable and parameters with the strength of fluctuation Δ .

Quantum yield:

The quantum yield [17], a measure of the efficiency of energy transport, can be written as

$$q = \frac{\sum_n k_{t,n} \tau_n}{\sum_n k_{t,n} \tau_n + \sum_n k_{d,n} \tau_n}, \quad (24)$$

where $\tau_n = \int_0^\infty \rho_{nn}(t) dt$ is the mean residence time for the population of the n -th site given by $\rho_{nn}(t)$. Next $k_{d,n}$ and $k_{t,n}$ are the decay constants for recombination and trap on the n -th site, respectively. Cao and Silbey [17] showed that the decay rate is necessary to be much smaller than the trapping rate, $k_{d,n} \ll k_{t,n}$ to obtain a high quantum yield. In such situation, the dependence of τ_n on $k_{d,n}$ can be neglected to give $\sum_n k_{t,n} \tau_n (k_{d,n} = 0) \approx 1$. Thus

$$q \approx \frac{1}{1 + \sum_n k_{d,n} \tau_n (k_{d,n} = 0)} = \frac{1}{1 + k_d \langle t \rangle}, \quad (25)$$

where the last form is obtained by setting the values of $k_{d,n}$ to be the same as k_d for all of the state n and with $\langle t \rangle = \sum_n \tau_n$.